

Dalton Transactions

Accepted Manuscript



This is an *Accepted Manuscript*, which has been through the Royal Society of Chemistry peer review process and has been accepted for publication.

Accepted Manuscripts are published online shortly after acceptance, before technical editing, formatting and proof reading. Using this free service, authors can make their results available to the community, in citable form, before we publish the edited article. We will replace this *Accepted Manuscript* with the edited and formatted *Advance Article* as soon as it is available.

You can find more information about *Accepted Manuscripts* in the [Information for Authors](#).

Please note that technical editing may introduce minor changes to the text and/or graphics, which may alter content. The journal's standard [Terms & Conditions](#) and the [Ethical guidelines](#) still apply. In no event shall the Royal Society of Chemistry be held responsible for any errors or omissions in this *Accepted Manuscript* or any consequences arising from the use of any information it contains.

COMMUNICATION

Synthesis, structural characterization, electronic spectroscopy, and microfluidic detection of Cu^{+2} and UO_2^{+2} [di-tert-butyl-salphenazine] complexes

Cite this: DOI: 10.1039/x0xx00000x

B. A. Maynard,^a J. C. Brooks,^a E. E. Hardy^a, C. J. Easley,^a and A. E. V. Gorden^{a*}

Received 00th January 2012,

Accepted 00th January 2012

DOI: 10.1039/x0xx00000x

www.rsc.org/

Metal templation by condensation of 2,3-diaminophenazine with 3,5-di-tert-butyl-2-hydroxybenzaldehyde around metal centers [M= Cu(II), and $\text{UO}_2(\text{VI})$] affords a new class of M[di-tert-butyl salphenazine] metal complexes. Reported here is the synthesis, single crystal X-ray structural characterization, electronic spectroscopy, and microfluidic detection of the formation of these M[di-tert-butyl salphenazine] complexes.

The lure of harnessing energy from the actinides is exciting as it provides one means to power generation without contributing to greenhouse gas emissions.¹ Currently, the positive aspects of this are counterbalanced by public perception of highly publicized radioactive material release events.² Interest in research regarding the actinide elements has increased in the last decade.^{1a, 3} Developing sensors that are able to selectively detect the presence of actinides in the environment is a key goal in rapid, immediate emergency response should release events occur *via* accident or incident.⁵ Our interest lies in the development of aromatic organic ligands for selective coordination of actinide ions, and to develop a microfluidic lab-on-a-chip to detect these metal complexes. Here, we have synthesized di-tert-butyl salphenazine [L] and two new metal complexes ($\text{Cu}[\text{L}]$, $\text{UO}_2[\text{L}]$), and we have characterized them in the solid state via single crystal X-ray diffraction (figure 1) and in the liquid phase *via* nuclear magnetic resonance, mass spectroscopy, and with UV and fluorescence spectroscopy. The UO_2^{+2} unit provides a reliable equatorial scaffold for templation of the planar aromatic ligand design, which has only previously been reported with zinc.⁶ Also reported is microfluidic sensing *via* a microspectrophotometer on sub-nanoliter droplets.

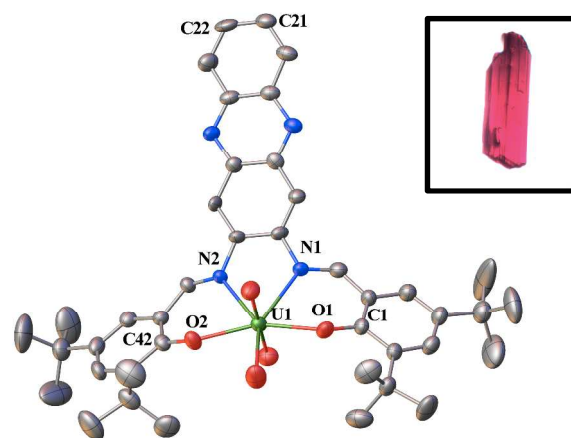


Figure 1 Projection of $\text{UO}_2[\text{L}]$ complex. Hydrogen atoms have been omitted for clarity. Inset image obtained on a CRAIC 20/20 PV microspectrophotometer shows the crystal after X-ray data collection.

Droplet generating microfluidic devices retain many advantages of standard microfluidics, while allowing the formation of discrete, monodispersed droplets at rates up to 100 kHz.^{4, 7} By producing isolated units at high rates, a statistically relevant testing population can be generated in under a minute. A principle tenet of *5f* chemistry is reduction of waste generation. This reduction, coupled with reduced assay costs and statistically relevant droplet scanning, make pairing the *5f* analysis and microfluidics ideal.⁷⁻⁸ An important comparison is copper, which is ten times more abundant in the earth's crust than uranium⁹, produced in asymmetric thermal fission [^{235}U and ^{239}Pu]¹⁰, and has been found to yield a false positive in systems designed as UO_2^{+2} sensors.¹¹

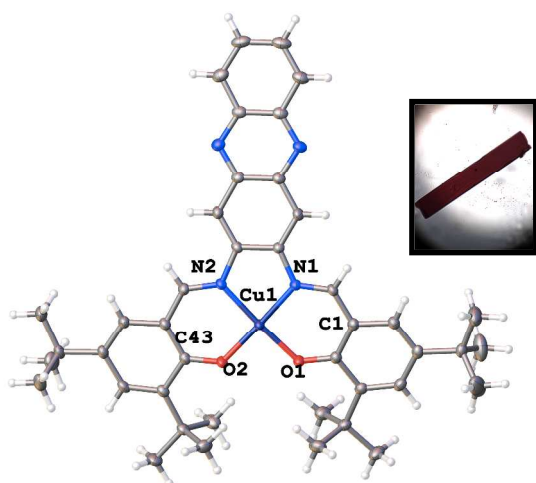


Figure 2 Projection of Cu[L] complex. Inset image obtained on the microspectrophotometer showing the crystal after X-ray data collection.

During metal templation, two 3,5-di-tert-butylsalicylaldehyde units and a 2,3-diaminophenazine unit undergo two condensation reactions around the metal center forming a tetradentate coordination pocket. The $\text{UO}_2[\text{L}]$ complex is shown in figure 1. Bond distances for the binding pocket can be found in table 1. U-N distances are found at 2.560(7) and 2.546(8) Å. U-O_{ligand} distances are found at 2.242(7) and 2.265(7) Å. Also in figure 3 is the mean (M) plane distance, which is defined as the distance the metal center is away from the plane generated by atoms C22-C23-O1-O2. For the $\text{UO}_2[\text{L}]$ complex this distance is 1.955 Å. The $\text{UO}_2[\text{L}]$ complex 360° rotation video in the supplemental information provides a pseudo-3d visualization.

The Cu[L] complex is shown in figure 2. Bond distances and angles for the binding pocket are found in table 1. Cu-N distances are found at 1.9304(16) and 1.9477(15) Å. Cu-O_{ligand} distances are found at 1.9091(12) and 1.8906(14) Å. For both the Cu^{+2} and UO_2^{+2} complexes the M-O and M-N bond distances agree with previously reported data.^{6, 12} For the Cu[L] complex, the M-plane distance is 0.171 Å. The Cu[L] complex 360° rotation video in the supplemental information provides a pseudo-3d visualization.

As the XRD atomic coordinate data indicates (illustrated numerically in table 1 and graphically in the M[di-tert-butylsalicylaldehyde] complex movies in the SI), the Cu complex more closely resembles a planar system as compared to the uranyl complex. In the electronic spectra of [L] (figure 3), two major features are observed in the UV-Vis range at 322 and 424 nm; ϵ

Table 1 Coordination pocket of [L] with bond distances between the coordinating atom and metal.

	Cu[L] Å	$\text{UO}_2[\text{L}]$ Å
M-N1	1.9304(16)	2.560(7)
M-N2	1.9477(15)	2.546(8)
M-O1	1.9091(12)	2.242(7)
M-O2	1.8906(14)	2.265(7)
N1-N2	2.603(2)	2.711(10)
O2-O1	2.6693(18)	4.422(10)

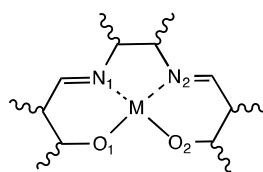


Figure 3 UV-Vis spectrum of the metal starting materials [Cu(NO₃)₂, UO₂(NO₃)₂], [L], Cu[L], and UO₂[L] complexes in pyridine at 20 μM.

$= 2.4 \times 10^4$ and 1.8×10^4 L mol⁻¹ cm⁻¹ respectively. The free base [L] was obtained by acid stripping the $\text{UO}_2[\text{L}]$ complex and used for further electronic spectroscopy characterization. Upon coordination of either metal centre, these two peaks are shifted to higher energy, and two charge transfer bands arise. The middle energy feature (364 nm) in the $\text{UO}_2[\text{L}]$ complex becomes a shoulder of the higher energy feature (336 nm). The predominant low energy feature in the $\text{UO}_2[\text{L}]$ complex has a maximum at 472 nm ($\epsilon = 1.9 \times 10^4$), with a shoulder at 520 nm. The Cu[L] complex, however, has a predominate peak at 522 nm ($\epsilon = 1.9 \times 10^4$), with a shoulder at 460 nm. The growth of these low energy peaks is visualized in the metal titration spectra (SI 1).

Thus, metal templation was used to form these two new metal complexes, Cu[L] and $\text{UO}_2[\text{L}]$, then characterized by X-ray diffraction. The structural data shows that upon ligand binding, the larger UO_2^{+2} unit perturbs the ligand from the expected aromatic planarity as compared to the smaller Cu^{+2} metal ion. The synthesis of the metal-ligand complexes, both the Cu^{+2} and UO_2^{+2} , represents unreported chemistry, and the electronic characterization shows that the aromatic M-L complexes have large molar extinction coefficients. Extending this fact leads to the novel application reported herein, namely the spectral detection of metal-ligand complexes in mere picoliter volumes (4×10^2 pL) on a microfluidic chip (figure 4).

Proof of concept for detection of these complexes within microfluidic droplets (pyridine droplets in perfluorocarbon oil) is shown in figure 4. Spectra collected using the microdroplet system match well with spectra from macro-scale measurements (SI2). Reducing sample volume by more than 6 orders of magnitude on this microchopper device⁴ with concurrent spectroscopic detection (figure 4C) could have reverberating effects within the field of environmental actinide sensing. By designing simple, easy-to-use devices, sample and waste volumes could be drastically reduced, while opening up the potential for on-site detection. The ability to reliably sense actinide elements at a release event and quickly respond could play a large role in altering the current standards of immediate response in field detection procedures.

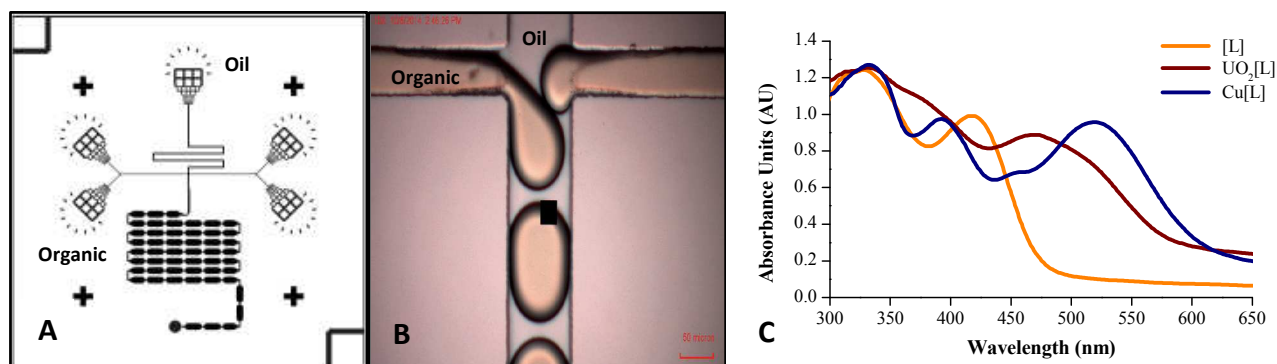


Figure 4 A. Droplet microchopper design. B. Oil and organic phases meet at a T-junction to form organic in oil droplets ($\text{UO}_2(\text{NO}_3)_2$ and ligand). C. CRAIC spectra of complexes collected on chip with $100\mu\text{m}$ optical path length¹¹

Conclusions

While current sensing methods for actinide elements have high selectivity and low limits of detection, they require large sample and reagent volumes and expensive instrumentation for assays that can take up to several days for the analysis to be completed.¹³ Our approach requires less than 5 minutes to collect multiple spectra and determine sample composition in picoliter volumes. This novel combination of droplet microfluidics with spectral detection using synthetic actinide sensors could help establish a foundation for research in microfluidic analysis of radioactive materials.

Notes and references

^a Department of Chemistry and Biochemistry, Auburn University, 179 Chemistry Building, Auburn, Alabama 36849, USA.

Funding for the microspectrophotometer was provided by a grant from the Auburn University Internal Grants Program to AEVG and the Department of Chemistry and Biochemistry. The microchip design was provided by Dr. Kennon S. Deal. This work was supported in part by the Defence Threat Reduction Agency, Basic Research Award # HDTRA1-11-1-0044 to Auburn University.

† Crystal data for $\text{Cu}[\text{di-tert-butylsal-phenazine}]$: $\text{Cu}[(\text{C}_{42}\text{H}_{48}\text{N}_4)_2]$ $M = 704.39$, Triclinic, space group $P\bar{1}$, $a = 9.9751(2)$, $b = 12.6630(3)$, $c = 14.8623(3)$, $\alpha = 93.610(1)^\circ$, $\beta = 96.835(1)^\circ$, $\gamma = 98.716(1)^\circ$, $V = 1836.17(7) \text{ \AA}^3$, $T = 180(2)^\circ\text{C}$, $Z = 2$, $\lambda = 0.71073 \text{ \AA}$, $\mu = 0.636 \text{ mm}^{-1}$, 7756 measured reflections, 6595 unique reflections, $R_{\text{int}} = 0.0333$, $R_1 [I > 2s(I)] = 0.0365$, $wR2$ (all data) = 0.0966, maximum/minimum residual electron density: 0.920 and $-0.420 \text{ e}^{-\text{\AA}^{-3}}$, CCDC 1019624.

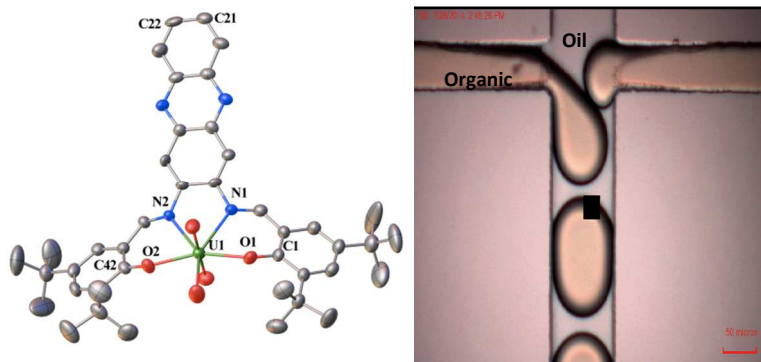
Crystal data for $\text{UO}_2[\text{di-tert-butylsal-phenazine}]$: $[\text{UO}_2(\text{C}_{42}\text{H}_{50}\text{N}_4\text{O}_5)(\text{OH}_2)] \cdot 1.5\text{C}_6\text{H}_8\text{O}$ $M = 1037.06$, Monoclinic, space group $P2_1/n$, $a = 18.0525(18)$, $b = 13.4858(13)$, $c = 20.817(2)$, $\beta = 97.379(3)^\circ$, $V = 5025.0(8) \text{ \AA}^3$, $T = 180(2)^\circ\text{C}$, $Z = 4$, $\lambda = 0.71073 \text{ \AA}$, $\mu = 3.278 \text{ mm}^{-1}$, 8404 measured reflections, 6341 unique reflections, $R_{\text{int}} = 0.0550$, $R_1 [I > 2s(I)] = 0.0717$, $wR2$ (all data) = 0.1427, maximum/minimum residual electron density: 2.544 and $-2.230 \text{ e}^{-\text{\AA}^{-3}}$, CCDC 1019622.

Electronic Supplementary Information (ESI) available: [Synthetic Methods, UV-Vis spectroscopic and titration data, crystallographic details

and movies of characterization by microspectrophotometer are included in the ESI]. See DOI: 10.1039/c000000x/

- (a) G. Tian and D. K. Shuh, *Dalton Trans.*, 2014, **43**, 14565; (b) IAEA Nuclear Technology Review, 2013, GC(57)/INF/2; (c) J. Johnson, *Chem. Eng. News*, 2014, **92**, 24.
- (a) V. H. M. Visschers and M. Siegrist, *Risk Analysis*, 2013, **33**, 333; (b) G. Hess, *Chem. Eng. News*, 2011, **89**, 10; (c) M. J. Goodfellow, H. R. Williams and A. Azapagic, *Energ. Policy*, 2011, **39**, 6199; (d) P. C. Burns, Y. Ikeda and K. Czerwinski, *MRS Bull.*, 2010, **35**, 868.
- (a) Y. Abe, Y. Iizawa, Y. Terada, K. Adachi, Y. Igarashi and I. Nakai, *Anal. Chem.*, 2014, **86**, 8521; (b) M. Roger, N. Barros, T. Arliguie, P. Thuéry, L. Maron and M. Ephritikhine, *J. Am. Chem. Soc.*, 2006, **128**, 8790; (c) M. Doran, A. J. Norquist and D. O'Hare, *Chem. Comm.*, 2002, 2946.
- K. S. Deal and C. J. Easley, *Anal. Chem.*, 2012, **84**, 1510.
- (a) A. Zaiter, B. Amine, Y. Bouzidi, L. Belkhir, A. Boucekkine and M. Ephritikhine, *Inorg. Chem.*, 2014, **53**, 4687; (b) A. E. Gorden, M. A. DeVore, and B. A. Maynard, *Inorg. Chem.*, 2013, **52**, 3445.
- G. Salassa, J. W. Ryan, E. C. Escudero-Adan and A. W. Kleij, *Dalton Trans.*, 2014, **43**, 210.
- R. Seemann, M. Brinkmann, T. Pfohl and S. Herminghaus, *Rep. Prog. Phys.*, 2012, **75**, 016601/1.
- (a) S.-Y. Teh, R. Lin, L.-H. Hung and A. P. Lee, *Lab Chip*, 2008, **8**, 198; (b) Y. Zhu and Q. Fang, *Anal. Chim. Acta*, 2013, **787**, 24.
- Z. Hu and S. Gao, *Chem. Geol.*, 2008, **253**, 205.
- P. Armbruster, M. Bernas, J. P. Bocquet, R. Brissot, H. R. Faust and P. Roussel, *Europhys. Lett.*, 1987, **4**, 793.
- J. L. Sessler, P. J. Melfi, D. Seidel, A. E. V. Gorden, D. K. Ford, P. D. Palmer and C. D. Tait, *Tetrahedron*, 2004, **60**, 11089.
- X. H. Wu, M. S. Bharara, T. H. Bray, B. K. Tate and A. E. V. Gorden, *Inorg. Chim. Acta*, 2009, **362**, 1847.
- J. H. Lee, Z. Wang, J. Liu and Y. Lu, *J. Am. Chem. Soc.*, 2008, **130**, 14217.

Graphical Abstract



Oil and organic phases meet at a T-junction in droplet microchip design to droplets. At left, Projection of UO_2 [di-tert-butyl salphenazine] complex